

SEE
622(21)
C21275



DEPARTMENT OF
ENERGY, MINES AND RESOURCES
MINES BRANCH
OTTAWA

THE MAGNETIC AND CERAMIC PROPERTIES
OF MIXED BARIUM-STRONTIUM FERRITES

SUTARNO, W. S. BOWMAN AND G. E. ALEXANDER

THE EFFECT OF FORMING PRESSURE AND
OF SINTERING TIME AND TEMPERATURE ON
THE MAGNETIC AND CERAMIC PROPERTIES
OF STRONTIUM FERRITE

SUTARNO, W. S. BOWMAN AND G. E. ALEXANDER

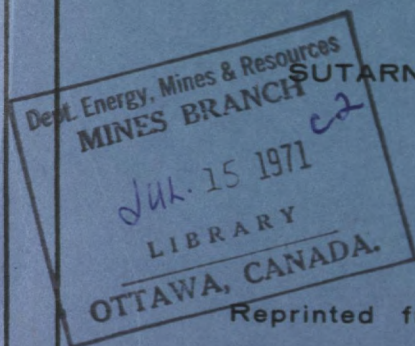
MINERAL SCIENCES DIVISION

Reprinted from the Journal of the Canadian Ceramic Society,

Volume 39, 1970

Reprint Series RS 102

Price 25 cents



© Crown Copyrights reserved

Available by mail from Information Canada, Ottawa
and at the following Information Canada bookshops

HALIFAX

1735 Barrington Street

MONTREAL

Æterna-Vie Building, 1182 St. Catherine St. West

OTTAWA

171 Slater Street

TORONTO

221 Yonge Street

WINNIPEG

Mall Center Bldg., 499 Portage Avenue

VANCOUVER

657 Granville Street

or through your bookseller

Price 25 cents Catalogue No. M38-8/102

Price subject to change without notice

Information Canada

Ottawa, 1971

The magnetic and ceramic properties of mixed barium-strontium ferrites

Sutarno*, W.S. Bowman** and G.E. Alexander***

ABSTRACT. The ceramic and magnetic properties of mixed barium-strontium ferrites having the composition $(\text{Ba}_{1-x}\text{Sr}_x)_0.52\text{Fe}_2\text{O}_3$, where $0 \leq x \leq 1$ and $\Delta x = 0.2$, have been studied. Anisotropic ferrite magnets with the above composition have been prepared and their green and sintered densities, diametral and thickness shrinkages, coercive force, remanent magnetization and maximum energy product have been measured and plotted as functions of their sintering temperatures and of their compositions. It was found that pure strontium ferrite ($x = 1$) has the best ceramic and magnetic properties in this system. An unexpectedly simple relationship was found to hold between the intrinsic coercive force and the density of all specimens.

Introduction

Hexaferrites having the chemical composition $\text{MO} \cdot n\text{Fe}_2\text{O}_3$, where M is Ba, Sr, Pb or a mixture thereof and n is either equal to or near 6.0, have been used successfully as the basic materials for the manufacture of ceramic permanent magnets. Not only can they be produced from relatively inexpensive raw materials, but also, this type of magnet has several properties that, for certain applications, are superior to those of metallic magnets. The ceramic permanent magnet has a high coercive force, high thermal and electrical resistivity and is chemically inert. At the same time, its maximum energy product $(BH)_{\text{max}}$ is still sufficiently high to be useful. The magnetic properties are derived from the anisotropic nature of the hexaferrite crystals. To take full advantage of this anisotropy, the crystallite particles of the ceramic magnet must be aligned so that their c-axes are parallel. This alignment can be obtained by the application of a magnetic field during the fabrication of the ceramic body⁽¹⁾.

Another important requirement for a good ceramic magnet is that it must be as dense as possible in order to have the greatest number of magnetic particles per unit volume, while, at the same time, its grain size must be maintained as small as possible in order to keep the coercive force high.

Various approaches have been used by a number of workers to prepare a dense, anisotropic, ceramic magnet with a small grain size. Most investigators used the doping technique to improve the ceramic properties of the ferrite. A large number of elements have been reported to improve the properties of ceramic ferrite magnets. Some were added to lower the calcination temperature⁽²⁾, while others were added as grain-growth inhibitors. Generally, the investigators' efforts to improve the properties of ferrite permanent magnets have been concentrated on the improvement of the ceramic properties, hoping simultaneously to improve the magnetic properties.

There are many variables that affect the ceramic properties of a ferrite magnet body. These variables can be divided into two main groups: (i) technological variables such as the method of preparation of the powder, calcination temperature, length of milling time, etc., and (ii) chemical variables, such as the Fe/M ratio, Ba:Sr:Pb

*Research Scientist; **Technical Officer; ***Electronics Technologist, Mineral Sciences Division, Mines Branch, Department of Energy, Mines and Resources, Ottawa, Canada.

proportions, and the concentration of minor constituents such as doping agents or impurities.

It is difficult to assess the importance of each of the variables individually to the final properties. Some of them, such as the $\text{Fe}_2\text{O}_3/\text{MO}$ ratio⁽³⁾, milling method and the particle size of the powder⁽⁴⁾, ⁽⁵⁾, and the method of preparation⁽⁶⁾, have important effects on the properties of the ceramic magnet body. In this work, the effect of Ba/Sr ratio on the magnetic and ceramic properties of mixed barium-strontium hexaferrites has been investigated.

Experimental procedures

1. General considerations

Several steps are required to prepare a ceramic magnet body. The effects of changes in some of these steps are interrelated. Ideally, one should study the effect of each variable on the properties of the product at each step. Because of the great number of variables involved in each step, an enormous volume of experimental work would be required. In the present work, in order to keep the volume of experimental work to a practical size, all the process variables were maintained as constant as possible. The only

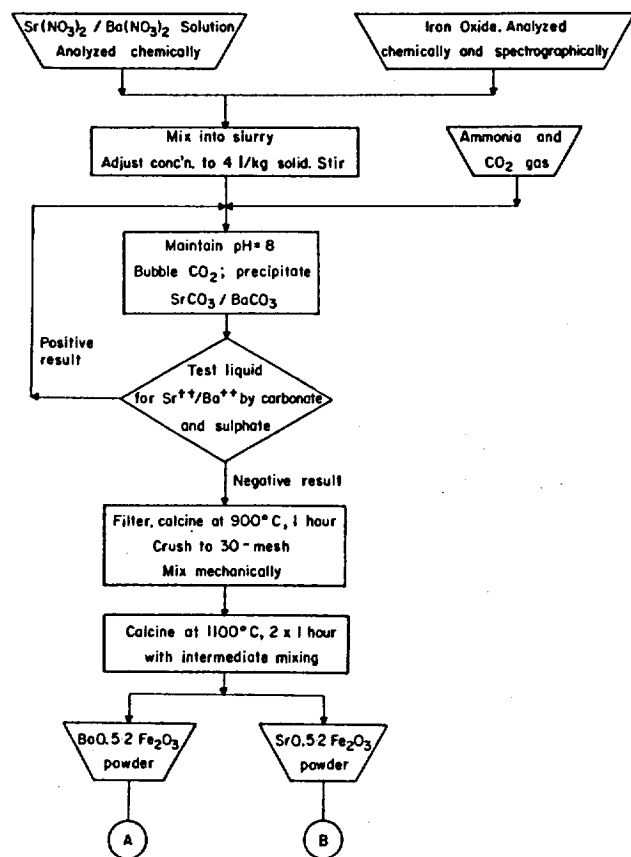


FIGURE 1A. Flow sheet for experimental investigation of ceramic and magnetic properties of barium/strontium ferrites (1st Section).

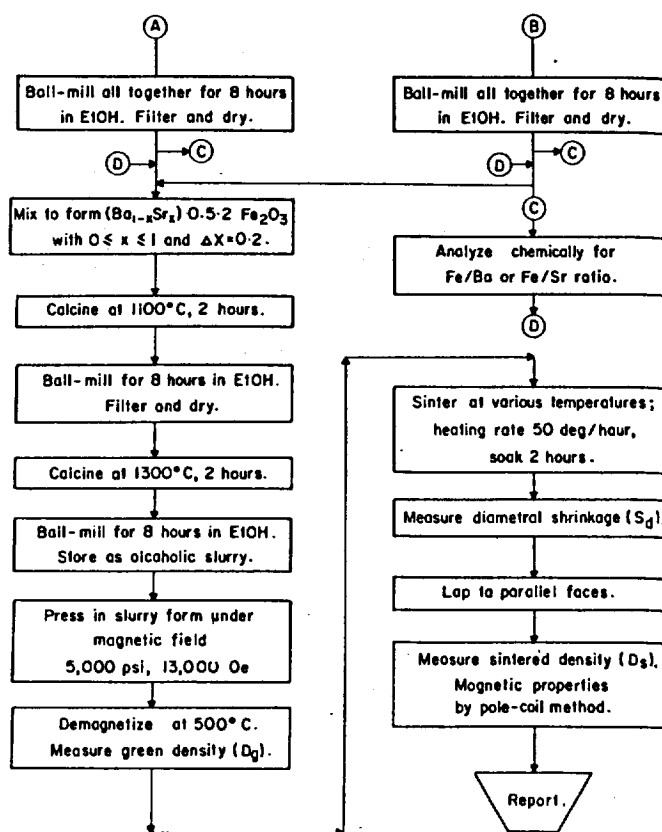


FIGURE 1B. Flow sheet for experimental investigation of ceramic and magnetic properties of barium/strontium ferrites (2nd Section).

variation was in the Ba/Sr ratio. The powders were prepared by the same method, using materials from the same sources, with calcination at the same temperature, soaking time and heating rate, with milling for the same length of time under the same milling conditions.

2. Sample preparation

The materials used in this work were reagent-grade iron oxide, barium nitrate, strontium nitrate, ammonia and carbon dioxide gas. No further purification was carried out on these raw materials. The iron oxide and the barium and strontium nitrate solutions were assayed chemically by standard methods⁽⁷⁾. The iron oxide was pre-dried at 150°C overnight.

The experimental procedure is illustrated schematically in Figures 1A and 1B. Appropriate amounts of iron oxide and barium/strontium nitrate solution to make $\text{Ba/SrO}_5\cdot 2\text{Fe}_2\text{O}_3$ were mixed to form a slurry. The size of each batch was about 2.5 kg. The ball-millings were carried out in ethanol in order to prevent the leaching of Ba and Sr from the samples that would occur if an aqueous milling medium were used. All but the first milling were carried out in an 8-inch-diameter mill, rotating at 72 rpm, using 1/2-inch-diameter balls. The weight ratios of sample: ethanol: balls were about 1:4:35. The first milling, which was intended only to homogenize the sample, was carried out in a 12-inch-diameter mill.

3. Fabrication

The ferrites, in the form of alcoholic slurries, were pressed under the influence of a magnetic field to form 1.5-inch-diameter discs⁽⁸⁾. The forming pressure was 5,000 psi. The magnetic field was applied intermittently with a maximum magnetomotive force of about 43,500 gilberts (34,600 amp-turns).

The "green" discs were then dried and demagnetized by heating them to 500°C. Their green densities (D_g) were determined from measurements of their dimensions and their weight.

4. Sintering

The sintering of these specimens was carried out in a large muffle furnace. Three or four equivalent discs of six batches, making 18 to 24 discs in total, were sintered at one time. The arrangement of the discs in the furnace was such that the effects of any variations in the hot zone of the furnace would be detected. The heating rate was set at 60 deg C/hr, the soaking time was 2 hr and the furnace was cooled to room temperature at its natural cooling rate.

The diameters of the sintered discs were measured to determine the diametral shrinkage (S_d). The discs were then lapped to perfect cylinders with their two faces parallel and their sintered densities (D_s) were determined prior to making the magnetic measurements. The parallel faces of the discs were ground with carborandum grinding compound No. 280. The faces were made parallel to within a tolerance of about ± 0.0002 inch.

It was not possible to measure the thickness shrinkage directly due to slight warping of some discs. The thickness shrinkage (S_t) was calculated as follows:

$$S_t = \left\{ 1 - \frac{D_g}{D_s} \left[\frac{1}{1 - S_d} \right]^2 \right\} \times 100$$

where S_t = thickness shrinkage in %, D_g = green density g/cm³, D_s = sintered density g/cm³, S_d = diametral shrinkage in %, ϕ_g and ϕ_s = green and sintered diameters, respectively, in cm.

5. Magnetic measurements

The magnetic properties of the specimens were measured using the "pole-coil" method⁽⁹⁾. The lapped discs were carefully placed between the two poles so as to minimize the air gap. A schematic diagram of the arrangement of the magnetic measurement equipment is given in Figure 2. Curves of $(B - H)$ vs. H were plotted automatically. The magnetic quantities B_r , iH_c , bH_c and $(BH)_{max}$ were read or calculated graphically. No corrections were made for any possible errors due to such factors as crystallographic and/or ceramic inhomogeneity of the specimens, non-linearity of the permeability of the pole

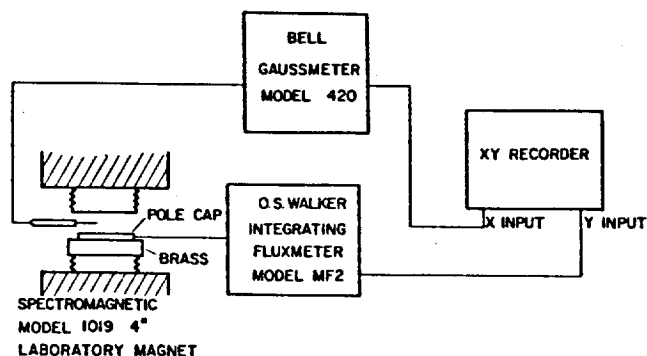


FIGURE 2. Schematic diagram of magnetic testing equipment for barium/strontium ferrites.

faces, etc. However, the quantities reported were obtained by averaging the measurements of three to four specimens.

Results and discussion

The chemical compositions of the end-members of this system were found to be $Ba_{0.5} \cdot 2Fe_2O_3$ and $Sr_{0.5} \cdot 2Fe_2O_3$, respectively. Since the other members of this system were prepared essentially by dry-mixing appropriate amounts of these two end-members, and since alcohol was used as the mixing medium, it is justifiable to assume that there was very little or no leaching of either barium or strontium from the samples during milling; that is, the $Fe_2O_3/(Ba + Sr)O$ ratio throughout the system was constant. The composition of the mixtures in the system can therefore be expressed as $(Ba_{1-x}Sr_x)_{0.5} \cdot 2Fe_2O_3$. Intervals of 0.2 in the various values of x were studied.

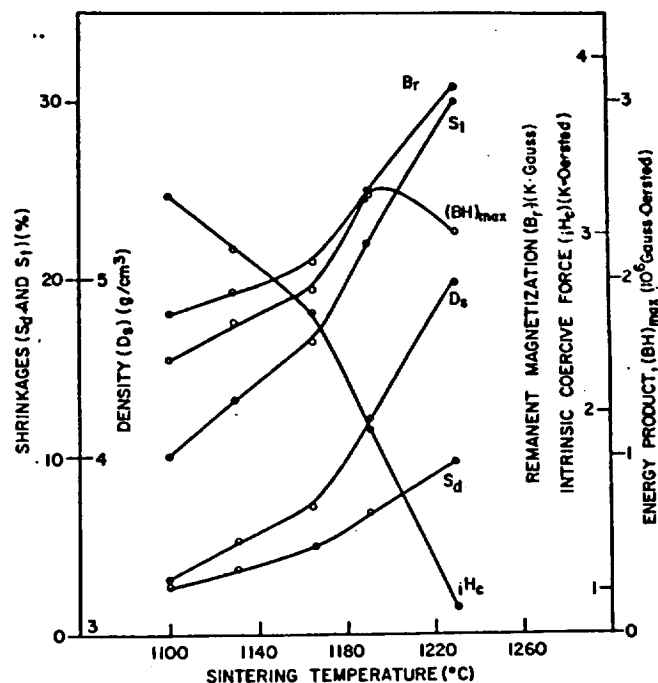


FIGURE 3A. Ceramic and magnetic properties of $Ba_{0.5} \cdot 2Fe_2O_3$, sintered at various temperatures for 2 hr.

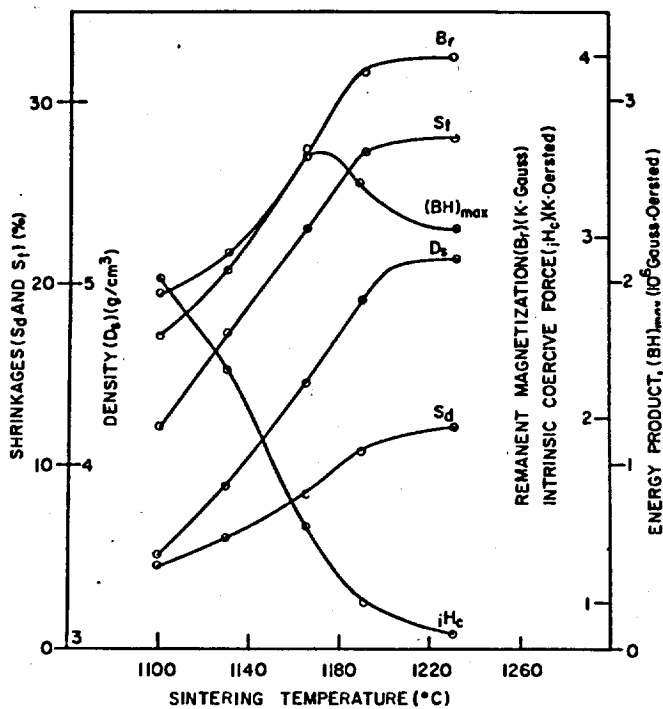


FIGURE 3B. Ceramic and magnetic properties of $(\text{Ba}_{0.8}\text{Sr}_{0.2})_{0.5} \cdot 2\text{Fe}_2\text{O}_3$, sintered at various temperatures for 2 hr.

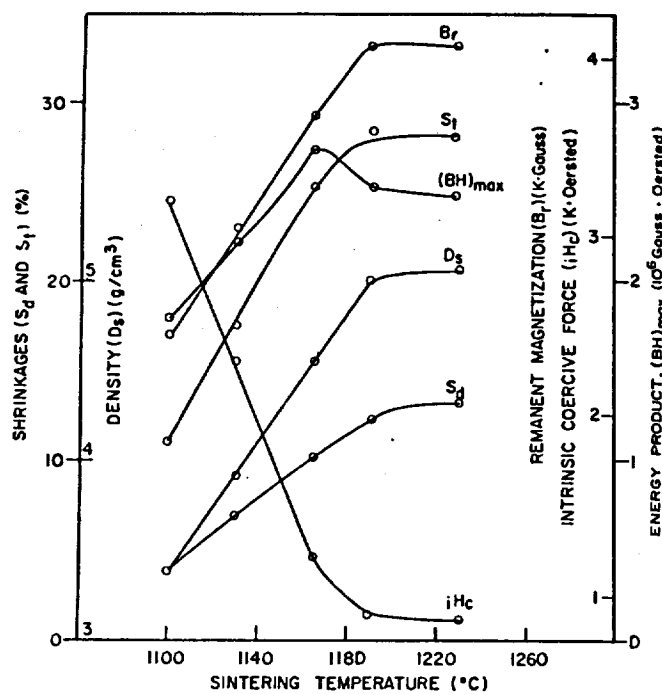


FIGURE 3D. Ceramic and magnetic properties of $(\text{Ba}_{0.4}\text{Sr}_{0.6})_{0.5} \cdot 2\text{Fe}_2\text{O}_3$, sintered at various temperatures for 2 hr.

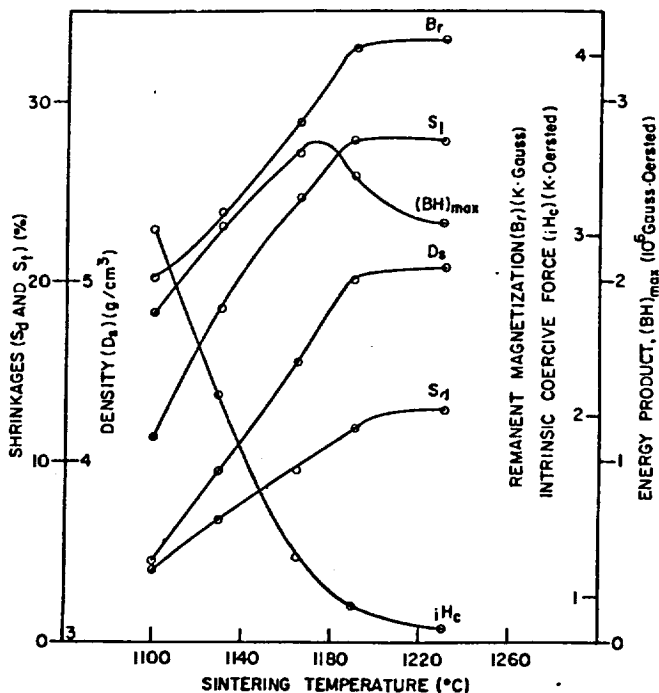


FIGURE 3C. Ceramic and magnetic properties of $(\text{Ba}_{0.6}\text{Sr}_{0.4})_{0.5} \cdot 2\text{Fe}_2\text{O}_3$, sintered at various temperatures for 2 hr.

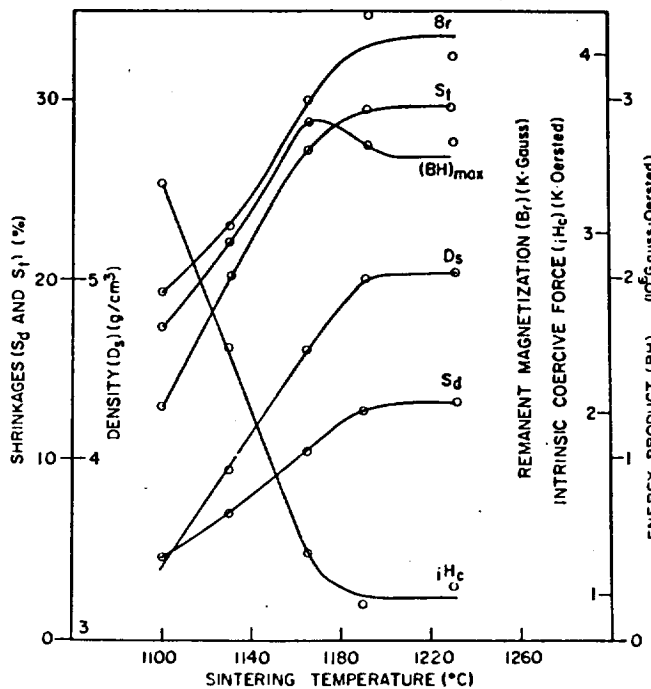


FIGURE 3E. Ceramic and magnetic properties of $(\text{Ba}_{0.2}\text{Sr}_{0.8})_{0.5} \cdot 2\text{Fe}_2\text{O}_3$, sintered at various temperatures for 2 hr.

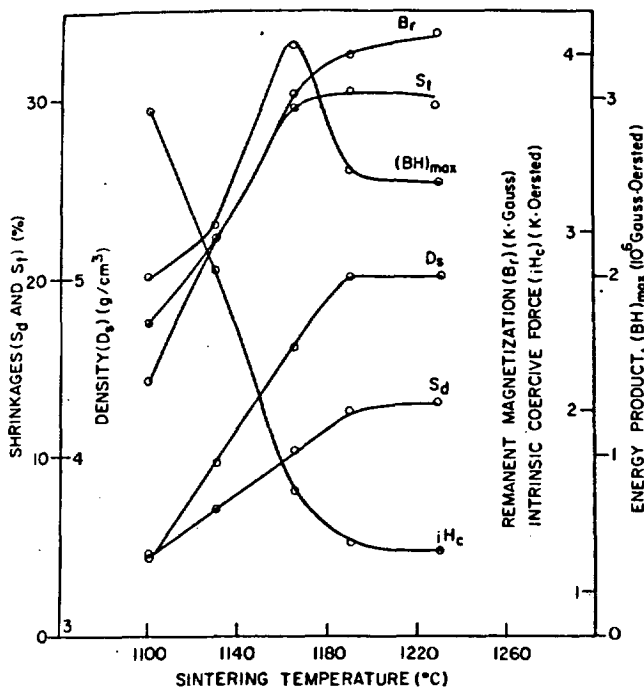


FIGURE 3F. Ceramic and magnetic properties of $\text{SrO} \cdot 0.5 \cdot 2\text{Fe}_2\text{O}_3$, sintered at various temperatures for 2 hr.

The results of both the ceramic and magnetic measurements on the series of compositions are shown graphically in Figures 3A to 3F inclusive. Recent investigations in this laboratory have shown that the operational variables, such as calcination temperature, milling time, forming pressure, etc. play an important role in the determination of the magnetic properties of hard ferrites(10), (11) and the conditions in the present study were not the optimum ones.

1. Density and shrinkages

It has been mentioned that the specimens in this system all have the chemical composition $(\text{Ba}_{1-x}\text{Sr}_x)\text{O} \cdot 0.5 \cdot 2\text{Fe}_2\text{O}_3$. The stoichiometric composition of the hexaferrites is $\text{MO} \cdot 0.6 \cdot \text{OFe}_2\text{O}_3$. There is a difference of opinion in the literature concerning the extent of solid solution of $\text{BaO} \cdot \text{Fe}_2\text{O}_3$ in $\text{BaO} \cdot 0.6 \cdot \text{OFe}_2\text{O}_3$. Y. Goto and T. Takada(12) reported that there was a considerable range of solid solution in the $\text{BaO} \cdot \text{Fe}_2\text{O}_3$ system in this regard. However, H.J. Van Hook(13) has denied this and claims that the range of solid solubility in the barium hexaferrite is either very narrow or non-existent. If $\text{BaO} \cdot 0.5 \cdot 2\text{Fe}_2\text{O}_3$ forms a single magnetoplumbite-type phase having the same lattice parameters as the stoichiometric hexaferrite, as stated by Goto and Takada, (implying the presence of lattice vacancies), it would have a density of 4.70 g/cm^3 . However, this cannot be the case, since a ceramic density of 4.96 g/cm^3 was obtained experimentally from this material

sintered at 1230°C for 2 hr. It is, therefore, considered far more probable that this material is, in fact, a solid solution of $\text{BaO} \cdot 0.6 \cdot \text{OFe}_2\text{O}_3$ and $\text{BaO} \cdot \text{Fe}_2\text{O}_3$. The proportion of the latter material required to give the correct gross composition is approximately 5%, by weight. This amount would barely be detectable by X-ray diffraction means. The density of $\text{BaO} \cdot \text{Fe}_2\text{O}_3$, using Goto and Takada's tetragonal cell parameters, would be approximately 6.0 g/cm^3 . The presence of 5% of this compound in a matrix of $\text{BaO} \cdot 0.6 \cdot \text{OFe}_2\text{O}_3$ would yield a theoretical density for $\text{BaO} \cdot 0.5 \cdot 2\text{Fe}_2\text{O}_3$ only slightly over that of the stoichiometric hexaferrite, viz., 5.352 g/cm^3 as against 5.314 g/cm^3 . If C. Okasaki, S. Mori and F. Kanamaru's hexagonal sub-unit cell parameters for $\text{BaO} \cdot \text{Fe}_2\text{O}_3$ (14) are used for this argument, the theoretical density of $\text{BaO} \cdot 0.5 \cdot 2\text{Fe}_2\text{O}_3$ would be 5.287 g/cm^3 .

The data for the strontium case are less complete but, if the second phase is $7\text{SrO} \cdot 5\text{Fe}_2\text{O}_3$, as claimed by Batti(15), then the proportion of this material that would need to be present in a matrix of $\text{SrO} \cdot 0.6 \cdot \text{OFe}_2\text{O}_3$ to give a gross composition of $\text{SrO} \cdot 0.5 \cdot 2\text{Fe}_2\text{O}_3$ would be approximately 3.5% by weight. This, also, would most probably not be detectable by X-ray diffraction means. In a similar way, the presence of this amount of $7\text{SrO} \cdot 5\text{Fe}_2\text{O}_3$ would give a theoretical density for the gross composition only slightly different from that of the stoichiometric hexaferrite.

Thus, no serious error can be encountered by assuming that the samples in the present study have theoretical densities lying between those of 100% stoichiometric $\text{BaO} \cdot 0.6 \cdot \text{OFe}_2\text{O}_3$ and 100% stoichiometric $\text{SrO} \cdot 0.6 \cdot \text{OFe}_2\text{O}_3$, on a linear basis depending on the degree of substitution of Ba by Sr.

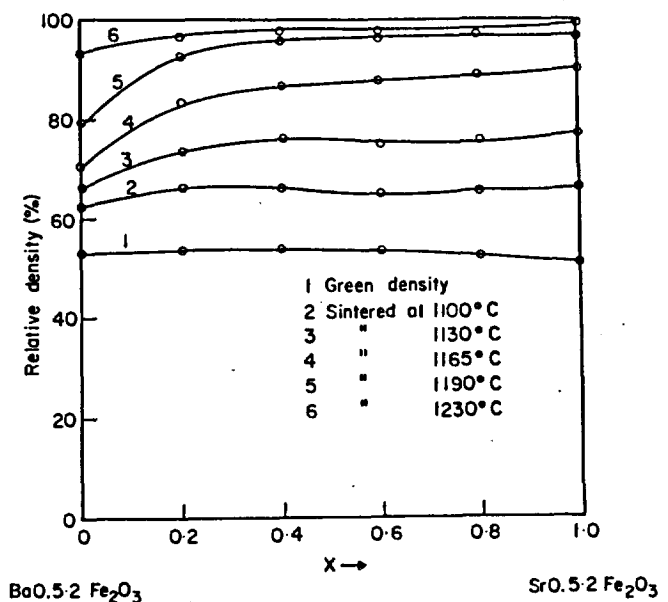


FIGURE 4. Relative sintered density of $(\text{Ba}_{1-x}\text{Sr}_x)\text{O} \cdot 0.5 \cdot 2\text{Fe}_2\text{O}_3$, sintered for 2 hr. at various temperatures.

The relative density, i.e., the ceramic density divided by the X-ray density of the same sample, as a function of the composition, is shown in Figure 4. It can be seen that the relative green density seems to be almost independent of the composition, varying only between 50 and 53%. The variation of the sintered density with sintering temperature is plotted, together with the magnetic properties, in Figures 3A to 3F, inclusive. The sintering temperature was varied up to 1230°C. At this temperature, the coercive force of all the samples was sufficiently low that there would be no advantage to sinter to higher temperatures.

The density of all the samples, with the exception of that of the pure barium ferrite, behaved in more or less the same way. It increased almost linearly as the sintering temperature was increased up to a certain point, beyond which the density changed very slowly with sintering temperature. This point occurred at a relative density of about 98-99%. The pure barium ferrite samples behaved differently from the others. The sintered density in this case increased relatively slowly with temperature up to about 1160°C, and then increased at a faster rate at temperatures higher than 1160°C. Figure 4 shows that only a small amount of strontium was needed to mask this different behaviour of barium ferrite. For $x > 0.2$, the densification behaviour was very similar for all samples.

These specimens all showed very strong anisotropic shrinkage behaviour. The shrinkage ratio (S_t/S_d) varied from 2.1 to 3.6 (Table I). Generally, the shrinkage ratio

decreased as the sintering temperature was increased.

2. Magnetic properties

The remanent magnetization, B_r , (Figures 3A to 3F inclusive) behaved as expected. It increases with sintering temperature in the same manner as the density. The corrected values of B_r , B_{r100} , are listed in Table II. B_{r100} is defined as the value of B_r when the density has been corrected to 100%, i.e., $B_{r100} = B_r/d$ relative.

It can be seen from this table that B_{r100} is essentially constant. Hence, the increase in the remanent magnetization with increasing sintering temperature is essentially the result of densification of the specimens. Any substantial improvement in the degree of orientation only occurs at the initial stage of sintering. There is no evidence of improvement in the degree of orientation over the range of sintering temperatures used in this work. The squareness of the hysteresis curves, however, showed substantial improvement with increasing sintering temperatures. This improvement may be mainly due to the disappearance of pores, which have a demagnetizing effect, lattice defects, etc., rather than to an improvement in degree of orientation. This assumption is based on the phenomenon observed by H.G. Richter and H.E. Dietrich⁽⁵⁾. They observed a lowering of the magnetic moment of a powder when it was subjected to extensive milling, a process known to introduce strain and lattice defects.

Table I - Ratio of thickness shrinkage to diametral shrinkage (S_t/S_d) for $(Ba_{1-x}Sr_x)O.5 \cdot 2Fe_2O_3$

Sintering temp. °C	COMPOSITION											
	x = 0		x = 0.2		x = 0.4		x = 0.6		x = 0.8		x = 1.0	
	S_t/S_d	Mean*	S_t/S_d	Mean	S_t/S_d	Mean	S_t/S_d	Mean	S_t/S_d	Mean	S_t/S_d	Mean
1100	3.72		2.97		2.70		2.97		3.14		2.84	
	3.27	3.40	2.83	2.90	2.61	2.73	2.58	2.83	2.28	3.09	2.76	2.78
	3.20				2.87		2.94		2.85		2.75	
1130	3.41		2.68		2.73		2.67		2.95		2.72	
	3.31	3.44	2.80	2.74	2.75	2.70	2.53	2.61	2.78	2.85	2.80	2.77
	3.59				2.61		2.62		2.81		2.80	
1165	3.32		2.59		2.55		2.55		2.65		2.57	2.45
	3.30	3.27	2.72	2.68	2.68	2.58	2.52	2.52	2.60	2.53	2.54	
	3.20		2.74		2.52		2.49		2.52		2.51	
1190	3.34		2.60		2.34		2.31		2.28		2.54	
	3.29	3.27	2.62	2.57	2.31	2.32	2.33	2.32	2.37	2.35	2.56	2.50
	3.28		2.53		2.31		2.31		2.39		2.45	
	3.16		2.54		2.34		2.33		2.35		2.45	
1230	3.06		2.32		2.12		2.08		2.23		2.11	2.11
	3.17	3.11	2.34	2.32	2.20	2.17	2.11	2.10	2.23	2.23	2.11	
	3.11		2.29		2.19		2.11		2.23		2.06	

*Mean: Arithmetic mean of (S_t/S_d).

Table II - Relative remanent magnetization* of $(\text{Ba}_{1-x}\text{Sr}_x)\text{O}\cdot 5\cdot 2\text{Fe}_2\text{O}_3$

Sintering temp. (°C)	COMPOSITION					
	x = 0	x = 0.2	x = 0.4	x = 0.6	x = 0.8	x = 1.0
1100	4093	4075	4205	4160	4102	4121
1130	4015	3959	4153	4087	3995	3900
1165	4034	4192	4195	4192	4209	4193
1190	4114	4217	4259	4254	4385	4184
1230	4080	4151	4223	4191	4122	4129

*Relative remanent magnetization = $B_r/100 = \frac{B_r}{d}$

Where d = relative density

Table III - Ratio of coercive forces bH_c/iH_c for $(\text{Ba}_{1-x}\text{Sr}_x)\text{O}\cdot 5\cdot 2\text{Fe}_2\text{O}_3$ at various sintering temperatures

Sintering temp. (°C)	COMPOSITION (x)					
	0	0.2	0.4	0.6	0.8	1.0
1100	0.73	0.86	0.83	0.79	0.77	0.69
1130	0.80	0.96	0.98	0.97	0.97	0.96
1165	0.96	0.98	0.98	0.99	0.99	0.98
1190	0.95	0.98	0.99	0.99	0.98	0.98
1230	0.99	0.98	0.98	0.99	0.98	0.97

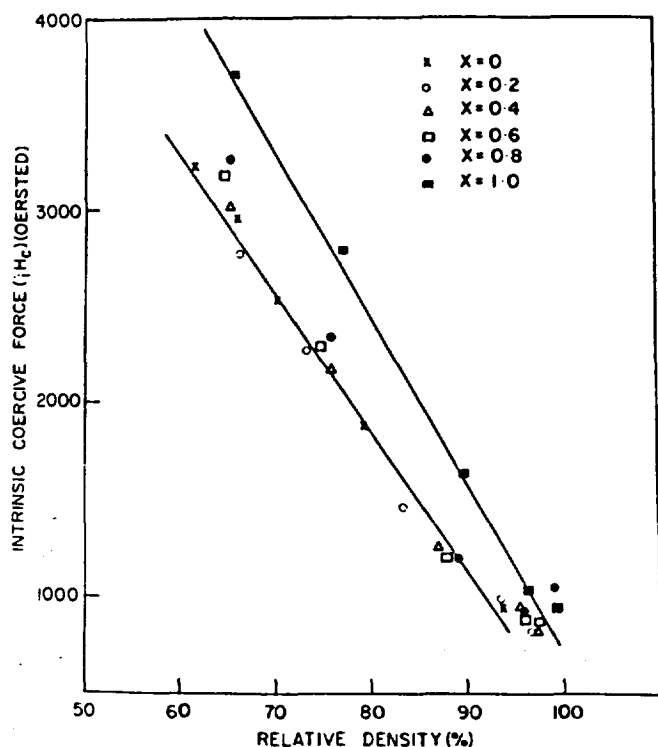


FIGURE 5. Intrinsic coercive force vs. relative density of $(\text{Ba}_{1-x}\text{Sr}_x)\text{O}\cdot 5\cdot 2\text{Fe}_2\text{O}_3$, calcined at 1300°C for 2 hr, ball-milled for 8 hr, and sintered at various temperatures for 2 hr.

The intrinsic coercive force behaved as expected. It decreased as the sintering temperature was increased. As is shown in Figure 5, this decrease in the intrinsic coercive

force appears to be approximately linear with respect to the increase in density. With the exception of the pure strontium composition ($x = 1$), all the points seem to fall on one straight line, especially those corresponding to relative densities of less than 90%. Pure strontium ferrite shows a higher intrinsic coercive force, but still yields a straight line of approximately the same slope. The least-squares fits of these lines are:

$$iH_c = -81.8d + 8394 \text{ with } \sigma = 109$$

for $x \leq 0.8$ and $d < 90$

and $iH_c = 84.6d + 9296$ with $\sigma = 63$
for $x = 1$ and $60 < d < 100$

where

iH_c = intrinsic coercive force in oersted,

d = relative density in %,

x = mole fraction of strontium ferrite,

$$\sigma = \sqrt{\frac{\sum (H_c - iH_c \text{ calc})^2}{n - 1}}$$

and n = number of experimental points.

The ratio of the coercive force, bH_c , to the intrinsic coercive force, iH_c , (Table III), which is one of the measures of the quality of the hysteresis curve of a specimen, is generally in the order of 96% to 99%, with the exception of those specimens with a very low remanent magnetization. For the latter specimens, the values of iH_c

are larger than the values of B_r and, consequently, the ratio of these two coercive forces does not measure the quality of the hysteresis curves.

As expected from the ceramic properties of these specimens, the optimum sintering temperature, from the point of view of the maximum energy product, $(BH)_{max}$, does not vary greatly over the range of specimens studied. This optimum occurred at about 1150°C, with the exception of pure barium ferrite, for which it occurred at about 1185°C. The optimum values of the maximum energy product, $(BH)_{max}$, are plotted against the composition in Figure 6. It can be seen that the optimum values of the maximum energy product vary from 2.5×10^6 gauss-oersted for pure barium ferrite to 3.3×10^6 gauss-oersted for pure strontium ferrite. These values are low compared with the best values attainable using both of these materials with doping and using undoped materials under different treatments. The first situation was obviously caused by the absence of grain-growth inhibitors and the second was caused by the choice of the technological variables which these investigators have found to be very important factors^{(10), (11)}.

The values of $(BH)_{max}$ for barium ferrite were lower than those for strontium ferrite. This is not unexpected since strontium ferrite has a higher anisotropic energy. The mixed-composition specimens, however, seem to exhibit a somewhat different behaviour. Their $(BH)_{max}$ values lie between the barium and strontium values, but they are virtually independent of the barium-to-strontium ratio.

There is a substantial difference between curve No. 1 (present work) and curve No. 2 (data replotted from Y.S. Borovik)⁽¹⁶⁾ in Figure 6 both in the values of the energy product and in their trends with respect to varying composition. Borovik obtained the optimum $(BH)_{max}$ value by sintering his specimens at 1230°C for 1 hr. This is almost 90°C higher than the optimum sintering temperature obtained in the present work. This difference is not surprising since his method of preparation, operational variables and Fe_2O_3/MO ratio were different from those used in this laboratory^{(3), (6), (10), (11)}.

Conclusions

From the foregoing discussion, the following conclusions can be drawn:

1. The relative green densities of the specimens seem to be independent of the Ba/Sr ratio. The barium ferrite specimens sintered at a higher temperature than their strontium counterparts. Mixed barium-strontium specimens, containing 20% or more strontium ferrite, behave in a manner similar to pure strontium ferrite.
2. The anisotropic properties of the hexaferrite discs were shown to vary strongly not only in their magnetic properties, but also in their ceramic properties. The ratio of the thickness to the diametral shrinkage (S_t/S_d) varies from 2.1 to 3.6. The understanding of this anisotropic behaviour is very important from the fabrication point of view.
3. The magnetic properties of the individual sample

compositions behaved as expected from their ceramic properties. The coercive force of all the samples was generally low. This was partly caused by insufficient milling time.

4. The pure strontium ferrite composition behaved somewhat differently from the mixed Ba-Sr compositions. It exhibited higher coercive force at a given density; consequently, it had higher energy products than other compositions. The coercive force of all the compositions, other than pure strontium ferrite, exhibited a straight line when plotted against relative density (up to 95% density). The coercive force of strontium ferrite specimens lay on a different straight line, but with similar slope.

5. The maximum energy products obtained in this work (with the process conditions as described in the experimental section) were 2.5×10^6 gauss-oersted for pure barium ferrite and 3.3×10^6 gauss-oersted for pure strontium ferrite. The energy products of samples of mixed Ba-Sr compositions fell between the above values, but the relationship between the energy product and the composition was not linear. This relationship was found to have different trends from those reported by Borovik (see Figure 6).

6. Contrary to the previously reported work by Borovik, pure strontium ferrite seems to have the best properties. This behaviour is caused not only by the fact that it has about 10% more anisotropic energy, but also that it sinters at a lower temperature than barium ferrite.

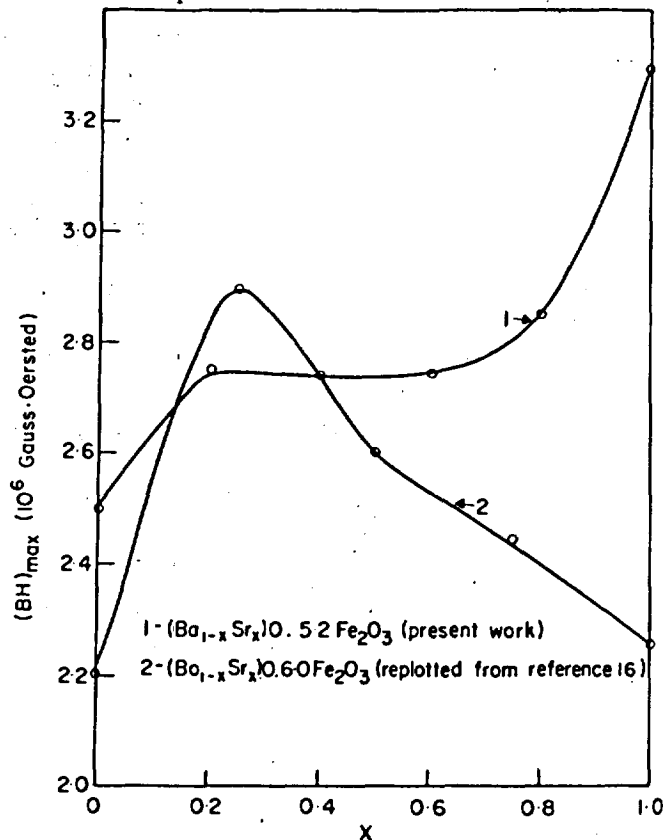


FIGURE 6. Energy product $(BH)_{max}$ vs. composition of $(Ba_{1-x}Sr_x)_{0.52}Fe_2O_3$ at their optimum sintering temperatures.

Acknowledgments

This work was conducted under the general direction of Dr. N.F.H. Bright, Head, Physical Chemistry Section, and partly supported in the early stages by the Defence Research Board of Canada under E.C.R.D.C. Project C-73.

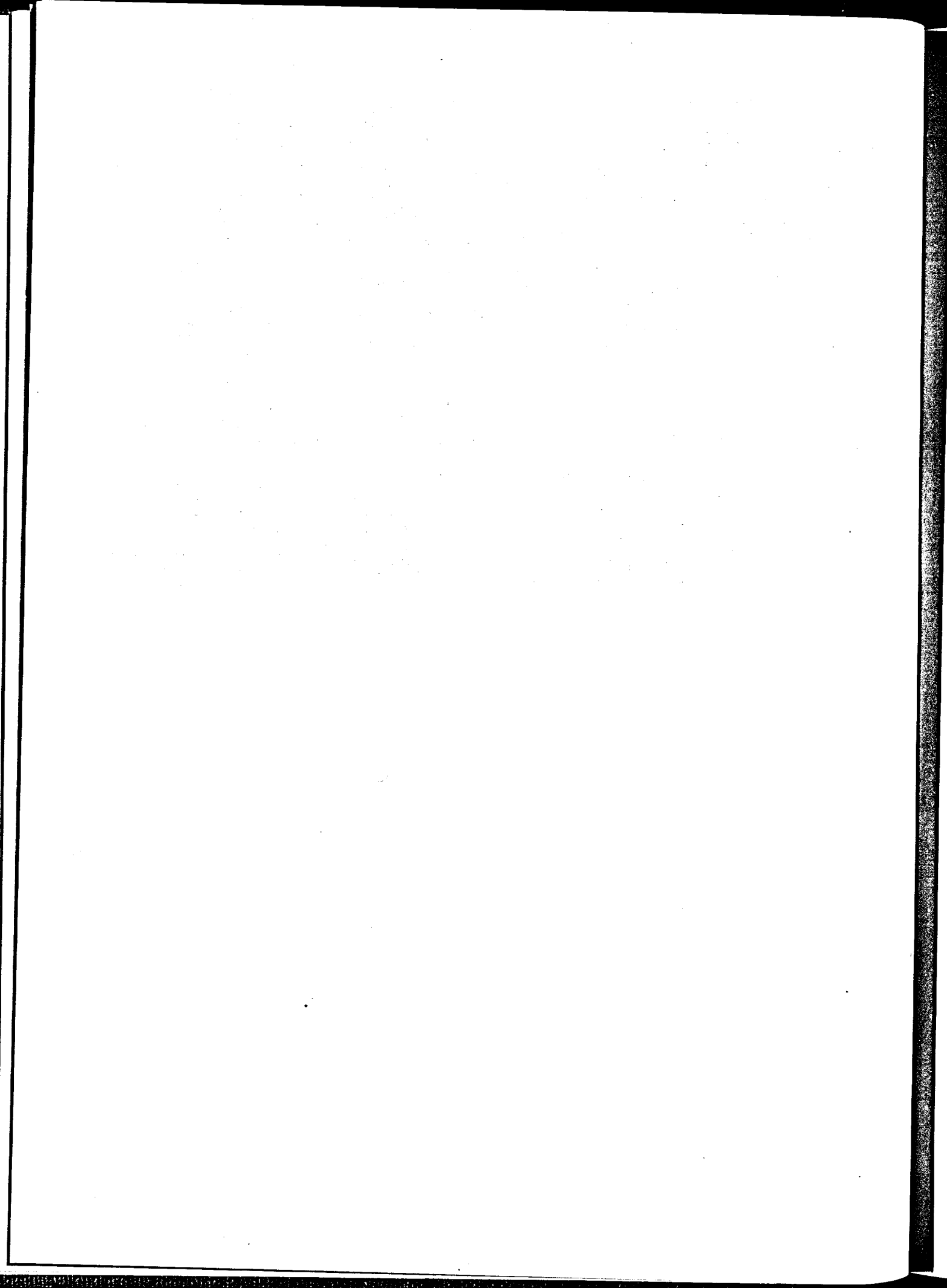
The lapping of the discs in preparation for making the magnetic measurements was carried out by the Preparation and Properties of Materials Section, Mineral Processing Division.

The authors would like to thank Dr. A.H. Webster for his valuable discussions throughout the period of the work and G.A.C. Wills for his experimental assistance.

The above-mentioned personnel are all members of the staff of the Mineral Sciences Division, Mines Branch.

References

1. Stuijts, A.L., G.W. Rathenau, and G.H. Weber. Ferroxdure II and III, anisotropic permanent magnet materials. *Philips Tech. Rev.* 16: 141-147, 1954.
2. Rola Company (Australia) Propriety Ltd. *Method of producing a permanent magnet material*. British Patent 1022969, March 16, 1966.
3. Stuijts, A.L. Sintering of ceramic permanent magnetic materials. *Trans. Brit. Ceram. Soc.* 35: 57-74, 1956.
4. Maurer, T.H., and H.G. Richter. Effect of milling methods on barium ferrite powder for the production of permanent magnets. *Powder Metallurgy*, 9(18): 151-162, 1966.
5. Richter, H.G., and H.E. Dietrich. On the magnetic properties of fine-milled barium and strontium ferrite. *J.E.E.E. Trans. on Magnetics, Mag-4 (2)*: 263-267, 1968.
6. Brown, C.S. The effect of ceramic technology on the properties of ferrites. *Proc. Brit. Ceram. Soc.* 19 (2): 55-72, 1964.
7. Vogel, A.I. A text-book of quantitative inorganic analysis. *John Wiley and Sons, New York, 3rd Ed.*, 1961.
8. Sutarno, W.S. Bowman, J.F. Tippons, and G.E. Alexander. Ferrites: Part III. Construction and operation of a magnetic orienting press for the fabrication of anisotropic ferrite magnets. *Mines Branch Investigation Report IR 67-46*, May 15, 1967.
9. Steingroever, E. Ein Magnetstahlprüfer mit richtkraftkompensiertem Flussmesser. *Archiv für Elektrotechnik*, 40: 275-279, 1952.
10. Sutarno, W.S. Bowman, G.E. Alexander, and J.D. Childs. The effect of some operational variables on the properties of strontium hexaferrite. *J. Can. Ceram. Soc.* 38: 9-13, 1969.
11. Sutarno, W.S. Bowman and G.E. Alexander. The effect of forming pressure and of sintering time and temperature on the magnetic and ceramic properties of strontium ferrite. See this issue, p. 45.
12. Goto, Y., and T. Takada. Phase diagram of the system BaO-Fe₂O₃. *J. Am. Ceram. Soc.* 43 (3): 150-153, 1960.
13. Van Hook, H.J. Thermal stability of barium ferrite (BaFe₁₂O₁₉). *J. Am. Ceram. Soc.* 47 (11): 579-581, 1964.
14. Okasaki, C., S. Mori, and F. Kanamaru. Magnetic and crystallographical properties of hexagonal barium mono-ferrite, BaO·Fe₂O₃. *J. Phys. Soc. Japan*, 16: 119, 1961.
15. Batti, P. Diagramma D'Equilibrio Del Sistema SrO-Fe₂O₃. *Annali di Chimica*, 52: 941-961, 1962.
16. Borovik, Y.S., and N.G. Yakovela. Influence of texture on the magnetic properties of mixed barium and strontium ferrites. *Fiz. Metal. Metalloved.*, 14 (6): 927-930, 1962.



The effect of forming pressure and of sintering time and temperature on the magnetic and ceramic properties of strontium ferrite

Sutarno*, W.S. Bowman** and G.E. Alexander***

ABSTRACT. The effects of certain processing variables on the ceramic and magnetic behaviour of pure, anisotropic, strontium ferrite ceramic magnets were investigated. It was found that the properties of the discs varied considerably with sintering temperature over the 1160°C to 1200°C range. The length of soaking time became less important as it was increased beyond two hours. The effect of forming pressure was less significant at the higher sintering temperatures. It was found that different combinations of these three variables could be employed to yield ceramic magnets having the same properties. It was also found that discs prepared under the same conditions from different batches of material could have different properties.

For the conditions employed in this study, the highest energy product achieved was 4.1×10^6 gauss-oersted with an intrinsic coercive force of 2000 oersted.

Introduction

The two main stages in the manufacture of a ferrite ceramic permanent magnet are the preparation of a suitable ferrite powder and the fabrication and sintering of the ceramic body. The final properties of the magnet are affected by the variables introduced in both stages. These variables may be chemical or operational in nature. An investigation of the effects of calcination temperature and milling time (operational variables in the first stage of manufacture) on the ceramic and magnetic properties of pure strontium ferrite has been previously reported⁽¹⁾. Hence, it was the purpose of the present investigation to study the effects of some of the operational variables in the second stage of manufacture, specifically, forming pressure, sintering temperature and soaking time.

Pure strontium ferrite with the nominal composition $\text{SrO} \cdot 5 \cdot 5\text{Fe}_2\text{O}_3$ was chosen as the material for study in the present work in order to be consistent with the previous work and because of its superior magnetic properties as compared with the other hexaferrites^{(2), (3), (4)}.

Because the first stage in the manufacture of a ferrite magnet involves solid-state processes to a large extent, there are some variables that, even in the laboratory, are difficult to control, and others that are not fully recognized. For this reason, the reproducibility between batches of material is a serious problem. In the present investigation, the extent of this problem was examined by determining the properties of aligned strontium hexaferrite magnets prepared from three batches of powder of the same nominal composition, size and preparation conditions.

Experimental procedures

The raw materials used in this work were reagent-grade strontium carbonate and iron oxide (hematite) powders. The spectrographic analyses of these powders are listed in Table I.

The experimental procedure is illustrated in the schematic diagram in Figure 1. For each of three batches, five pounds of iron oxide powder were mixed with the appropriate amount of strontium carbonate to yield the composition $\text{SrO} \cdot 5 \cdot 5\text{Fe}_2\text{O}_3$. The mixing was done in a rod mill using an alcohol medium in place of water in order to

*Research Scientist; **Technical Officer; ***Electronics Technologist, Mineral Sciences Division, Mines Branch, Department of Energy, Mines and Resources, Ottawa, Canada.

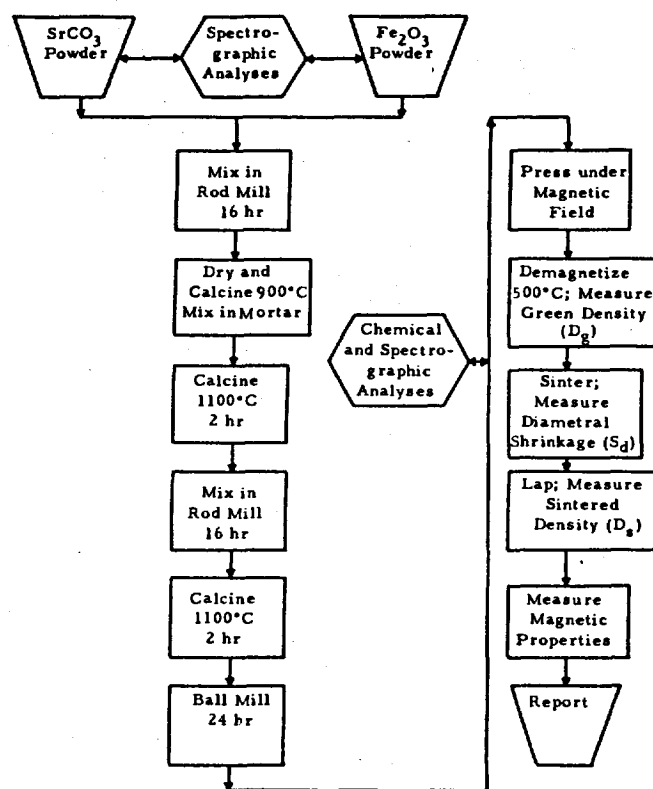


FIGURE 1. Schematic diagram of the experimental procedure.

guard against possible strontium loss by solution. After batch calcination, the masses were ball-milled in an 8 in. diameter steel mill using 3/8 in. diameter steel balls. The mass ratio of ferrite:alcohol:balls was 1:4:35.

Discs, 1.5 in. in diameter, were pressed under a magnetic field of approximately 13,000 oersted from the ferrite slurries⁽⁵⁾. The forming pressures, which were read on a calibrated hydrostatic pressure gauge, were 2,500, 5,000, and 10,000 psi.

The discs from batch No. 1 were sintered in an electrically-heated tube furnace in an oxygen atmosphere at 1160°C, 1180°C and 1200°C. Discs from batch Nos. 2 and 3 were sintered at 1200°C only. The heating rate was 100 deg C per hour and the soaking times were from 0 to 360 minutes; the specimens were cooled at the natural rate of the furnace. The discs were lapped to cylinders with their faces parallel to within 0.0002 in. using silicon carbide grinding compound, grade 600.

Densities of the lapped discs were determined from their weights and dimensions. Values of the thickness shrinkage (S_t) were calculated from the "green" densities (D_g), sintered densities (D_s) and diametral shrinkages (S_d) since slight warping made direct measurement difficult.

The magnetic properties of the specimens were measured by the "pole-coil" method⁽⁶⁾. ($B-H$) vs. H curves were plotted automatically and the intrinsic coercive force (H_c), coercive force (bH_c), remanent

magnetization (B_r) and maximum energy product $[(BH)_{max}]$ were measured graphically. Each disc was measured in five places in order to average out local vibrations.

Results and discussion

The spectrographic analyses of the raw materials and the ferrite powders are given in Table I. It can be seen that the processing did not introduce any significant amounts of impurities into the three batches of ferrite material. Also, chemical analysis of batch Nos. 1, 2 and 3 showed that the compositions were $SrO.5.73Fe_2O_3$, $SrO.5.77Fe_2O_3$ and $SrO.5.76Fe_2O_3$, respectively. It can be said, therefore, that these batches of material have the same composition and are of "reagent-grade" purity.

Table I. Semi-quantitative spectrographic analysis of raw materials and strontium ferrite (Wt.%)*

Elements	SrCO ₃	Fe ₂ O ₃	Strontium Ferrite		
			Batch No. 1	Batch No. 2	Batch No. 3
Ba	—	ND	ND	ND	ND
B	ND	—	ND	ND	ND
Mn	ND	0.06	0.02	0.02	0.02
Sb	ND	ND	ND	ND	ND
Mg	ND	0.04	0.01	0.01	0.01
As	ND	—	ND	ND	ND
Mo	ND	ND	ND	ND	ND
W	ND	ND	ND	ND	ND
Pb	ND	ND	ND	ND	ND
Sn	ND	ND	ND	ND	ND
Cr	ND	ND	0.03	0.03	0.03
Si	0.03	0.03	ND	ND	ND
Nb	ND	—	ND	ND	ND
Ta	ND	—	ND	ND	ND
Fe	ND	PC	PC	PC	PC
Ge	ND	—	ND	ND	ND
Bi	ND	ND	ND	ND	ND
Al	ND	0.006	0.01	0.04	0.02
In	ND	—	ND	ND	ND
Zr	ND	ND	ND	ND	ND
Cu	ND	0.01	ND	ND	ND
Ag	ND	ND	ND	ND	ND
Na	ND	ND	ND	ND	ND
Zn	ND	ND	ND	ND	ND
Ti	ND	ND	ND	ND	ND
Ni	ND	0.03	ND	ND	ND
Co	ND	ND	ND	ND	ND
Sr	PC	ND	PC	PC	PC
Ca	0.07	—	ND	ND	ND

*ND - Non detectable; PC - Principal constituent.

Table II. Ceramic and magnetic properties of strontium ferrite

Batch No.	Forming pressure (P) (psi)	Green density (D_g) (g/cm^3)	Sintering temp. ($^{\circ}C$)	Soak time (min)	Diametral shrinkage (S_d) (%)	Thickness shrinkage (S_t) (%)	B/A	Sintered density (D_s) (g/cm^3)	Remanent magnetization (B_r) (gauss)		Intrinsic coercive force (H_c) (oersted)		Coercive force (H_c) (oersted)		Maximum energy product ($(BH)_{max}$) (10^6 gauss-oersted)	
									Mean	Std.Dev.	Mean	Std.Dev.	Mean	Std. Dev.	Mean	Std. Dev.
1	2500	2.66	1200	30	11.8	29.3	0.803	4.83	3806	33	2186	30	2168	23	3.44	0.05
1	5000	2.83	1200	30	10.9	26.7	0.823	4.87	3892	30	2116	9	2098	11	3.58	0.05
1	10000	2.92	1200	30	10.1	25.8	0.825	4.87	3884	33	2132	18	2112	18	3.55	0.03
1	2500	2.66	1200	120	11.9	30.9	0.784	4.97	4120	0	1688	27	1658	18	3.89	0.01
1	5000	2.82	1200	120	10.9	28.8	0.799	4.98	4066	19	1612	23	1592	22	3.75	0.04
1	10000	2.93	1200	120	10.0	27.2	0.809	4.98	4060	19	1628	18	1612	16	3.71	0.06
1	2500	2.68	1200	240	11.8	30.8	0.785	4.98	4136	9	1400	14	1384	17	3.59	0.02
1	5000	2.83	1200	240	10.8	29.3	0.793	5.02	4152	18	1376	15	1358	11	3.59	0.03
1	10000	2.95	1200	240	10.1	27.2	0.810	5.01	4182	18	1368	11	1358	11	3.65	0.03
1	2500	2.59	1200	360	12.1	32.6	0.767	4.96	4150	29	1344	17	1328	11	3.58	0.06
1	5000	2.77	1200	360	11.2	29.6	0.792	4.98	4180	45	1312	13	1296	17	3.58	0.04
1	10000	2.88	1200	360	10.3	28.7	0.795	5.01	4214	24	1212	18	1202	20	3.42	0.06
1	2500	2.59	1180	0	10.2	23.4	0.853	4.19	3088	11	3576	26	2818	18	2.22	0.03
1	5000	2.72	1180	0	9.9	22.7	0.858	4.33	3204	22	3468	50	2976	33	2.40	0.02
1	10000	2.90	1180	0	8.2	23.4	0.834	4.49	3350	20	3260	27	3090	39	2.61	0.04
1	2500	2.59	1180	120	11.5	28.9	0.803	4.65	3600	28	2554	26	2526	25	3.05	0.04
1	5000	2.73	1180	120	10.6	27.6	0.810	4.72	3606	13	2494	32	2454	29	3.11	0.04
1	10000	2.90	1180	120	9.9	25.2	0.840	4.78	3696	9	2426	19	2400	16	3.19	0.02
1	2500	2.58	1180	240	11.9	29.7	0.798	4.73	3732	27	2306	44	2280	40	3.30	0.06
1	5000	2.74	1180	240	11.2	27.9	0.812	4.82	3814	19	2186	51	2168	52	3.49	0.02
1	10000	2.92	1180	240	10.4	25.7	0.829	4.89	3896	43	2100	24	2082	20	3.57	0.09
1	2500	2.60	1180	360	11.5	30.1	0.790	4.76	3796	51	2174	51	2150	45	3.45	0.07
1	5000	2.72	1180	360	11.0	28.5	0.803	4.79	3808	33	2176	25	2150	20	3.46	0.08
1	10000	2.94	1180	360	10.0	25.5	0.828	4.87	3872	18	2052	23	2032	23	3.55	0.07
1	2500	2.56	1160	30	9.9	20.7	0.880	3.98	2860	17	3844	34	2646	9	1.90	0.01
1	5000	2.70	1160	30	9.5	20.3	0.881	4.13	2966	19	3698	29	2740	20	2.06	0.04
1	10000	2.91	1160	30	8.9	19.1	0.899	4.34	3120	0	3474	25	2856	5	2.28	0.00
1	2500	2.57	1160	120	11.0	24.6	0.847	4.30	3192	18	3226	32	2948	33	2.38	0.04
1	5000	2.71	1160	120	10.5	23.3	0.857	4.41	3264	17	3124	42	2990	30	2.48	0.03
1	10000	2.85	1160	120	9.9	23.1	0.857	4.57	3376	22	2988	45	2958	52	2.65	0.05
1	2500	2.56	1160	240	11.6	26.4	0.833	4.45	3344	22	2894	33	2868	30	2.61	0.04
1	5000	2.68	1160	240	10.8	25.4	0.836	4.53	3400	0	2852	33	2808	27	2.70	0.00
1	10000	2.87	1160	240	10.1	23.7	0.856	4.65	3482	4	2760	34	2734	34	2.82	0.01
1	2500	2.54	1160	360	11.6	27.1	0.825	4.46	3400	0	2818	28	2792	23	2.70	0.00
1	5000	2.70	1160	360	10.8	25.3	0.837	4.54	3440	0	2760	29	2732	19	2.77	0.04
1	10000	2.87	1160	360	10.1	23.9	0.846	4.66	3524	33	2674	11	2656	9	2.90	0.02
2	2500	2.60	1200	30	8.6	28.1	0.787	4.33	3600	0	3012	36	2964	55	3.13	0.03
2	5000	2.73	1200	30	8.0	27.0	0.793	4.42	3732	30	2906	9	2884	9	3.32	0.04
2	10000	2.92	1200	30	7.2	24.6	0.813	4.50	3726	65	2830	41	2794	44	3.32	0.04
2	2500	2.60	1200	120	9.4	32.5	0.745	4.69	4060	71	2118	48	2090	39	3.92	0.10
2	5000	2.71	1200	120	8.7	31.8	0.747	4.77	4032	59	2008	54	1954	66	3.86	0.12
2	10000	2.88	1200	120	8.2	29.3	0.770	4.83	4168	29	1838	44	1784	38	4.05	0.08
2	2500	2.59	1200	240	9.7	33.7	0.734	4.79	4126	19	1812	16	1794	24	4.05	0.06
2	5000	2.74	1200	240	8.8	31.9	0.747	4.84	4185	36	1656	30	1640	37	4.01	0.02
2	10000	2.87	1200	240	7.9	30.3	0.757	4.85	4154	51	1704	70	1682	77	3.97	0.03
2	2500	2.61	1200	360	9.3	34.3	0.724	4.84	4200	0	1588	36	1576	35	3.93	0.04
2	5000	2.73	1200	360	8.7	33.8	0.736	4.88	4256	44	1472	62	1456	59	3.87	0.04
2	10000	2.89	1200	360	8.0	30.3	0.758	4.90	4238	27	1492	77	1480	74	3.85	0.05
3	2500	2.63	1200	30	7.2	25.1	0.807	4.07	3366	70	3700	112	3206	56	2.72	0.11
3	5000	2.77	1200	30	6.7	24.1	0.814	4.19	3468	74	3588	107	3284	9	2.90	0.12
3	10000	2.92	1200	30	6.5	23.8	0.815	4.39	3632	61	3326	120	3190	106	3.19	0.15
3	2500	2.65	1200	120	7.8	29.9	0.760	4.45	3770	72	2772	114	2656	104	3.42	0.14
3	5000	2.77	1200	120	7.3	29.1	0.765	4.55	3836	70	2690	89	2602	89	3.58	0.16
3	10000	2.94	1200	120	6.9	27.4	0.788	4.67	3928	70	2524	114	2446	134	3.72	0.12
3	2500	2.61	1200	240	8.5	33.3	0.729	4.68	4040	75	2308	139	2232	154	3.92	0.11
3	5000	2.78	1200	240	7.8	30.9	0.749	4.73	4060	60	2154	100	2104	111	3.92	0.13
3	10000	2.95	1200	240	7.4	28.6	0.771	4.87	4168	44	2014	93	1956	84	4.06	0.05
3	2500	2.64	1200	360	8.7	33.3	0.731	4.75	4056	46	2008	159	1950	179	4.08	0.05
3	5000	2.76	1200	360	8.9	32.1	0.738	4.80	4192	52	1932	173	1850	149	4.03	0.10
3	10000	2.96	1200	360	7.4	28.9	0.768	4.87	4200	40	1808	102	1772	96	4.02	0.02

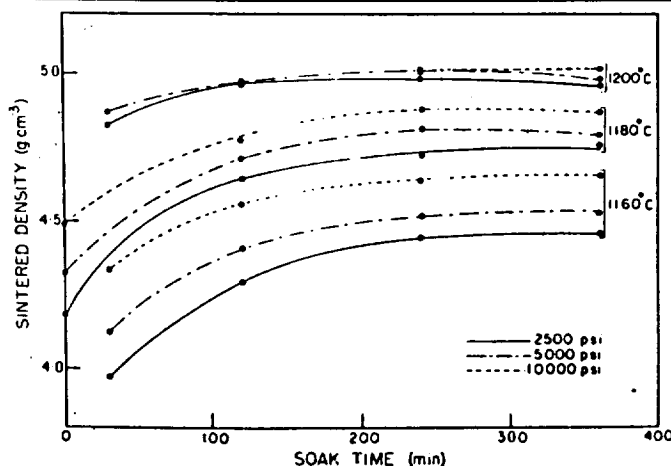


FIGURE 2. Effect of soak time, forming pressure and sintering temperature on the sintered density of strontium ferrite (batch no. 1).

The ceramic and magnetic properties of all discs prepared in the present investigation are listed in Table II and are shown graphically as functions of soaking time in Figures 2 to 9. As mentioned earlier, the magnetic properties of each disc were measured in five places. The average values and standard deviations are reported in Table II.

Figure 2 shows the effect of sintering temperature, soaking time and of forming pressure on the sintered density of specimens prepared from batch No. 1. The sintering temperature has the greatest effect on the density. The soaking time has a strong effect for short times, but the values approach an asymptote beyond 200 minutes. This limit is dependent on both sintering temperature and forming pressure. The effect of forming pressure diminishes as the process of densification progresses. Specimens sintered for 360 minutes at 1180°C could barely achieve the density of those sintered for only 30 minutes at 20

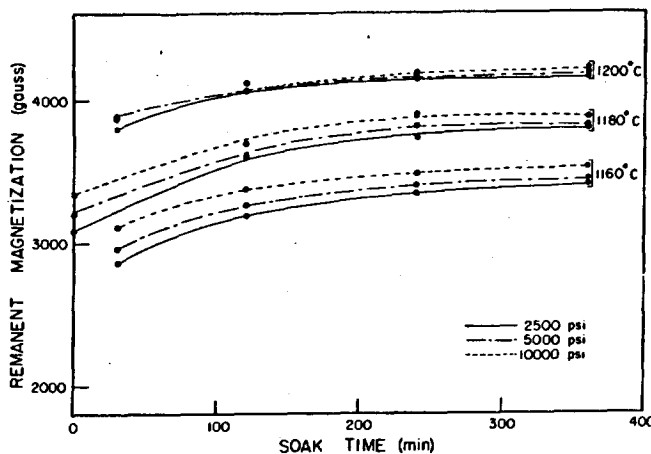


FIGURE 3. Effect of soak time, forming pressure and sintering temperature on the remanent magnetization of strontium ferrite (batch no. 1).

degrees higher. This behaviour will influence the design and scheduling of industrial kilns used for sintering such materials.

Figure 3 shows that sintering temperature, soaking time and forming pressure affect the remanent magnetization in much the same way as they affect the

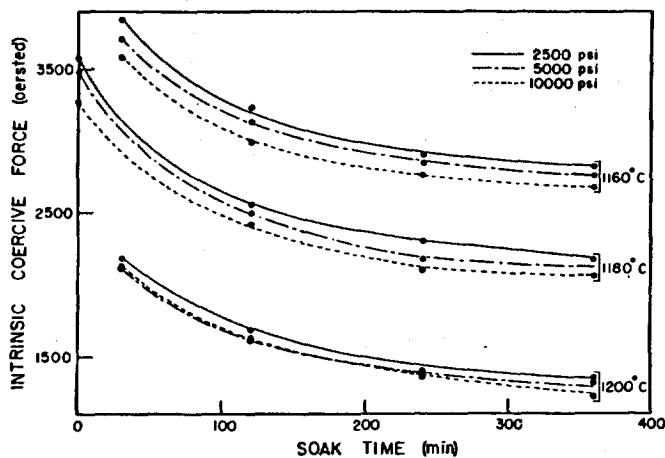


FIGURE 4. Effect of soak time, forming pressure and sintering temperature on the intrinsic coercive force of strontium ferrite (batch no. 1).

sintered density. It can be seen that a sintering temperature of higher than 1180°C is required to achieve a remanent magnetization of 4000 gauss or higher.

The behaviour of the intrinsic coercive force with respect to these variables is the reverse of that of the density. As is shown in Figure 4, it decreases as the sintering temperature, soaking time and forming pressure are increased. The rate of change of intrinsic coercive force with respect to change of sintering temperature and of soaking time would seem to be greater than the rate of

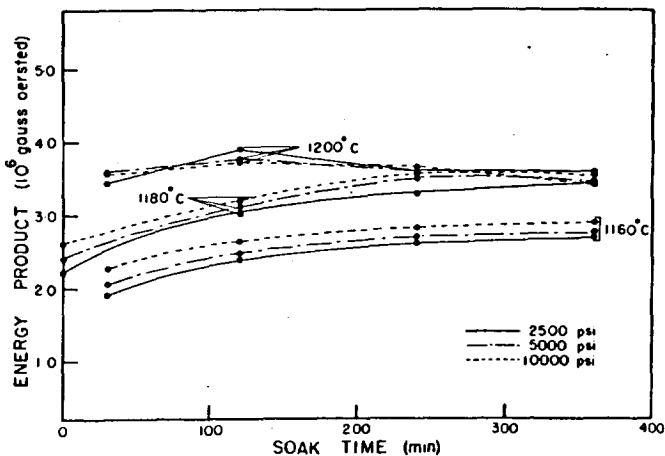


FIGURE 5. Effect of soak time, forming pressure and sintering temperature on the maximum energy product of strontium ferrite (batch no. 1).

change of remanence. However, the effect of forming pressure is of the same order of magnitude for both properties.

Figure 5 shows the effect of these variables on the maximum energy products of the specimens prepared from batch No. 1. Since the hysteresis curves obtained in this work were all reasonably rectangular, the maximum energy product of a specimen is dependent only on its remanent magnetization and its intrinsic coercive force. Moreover, if the intrinsic coercive force is greater than half of the remanence, the maximum energy product is dependent only on the remanence. Hence, for the discs sintered at 1160°C and 1180°C, the $(BH)_{max}$ curves are very similar to the remanent magnetization curves in Figure 3. At a sintering temperature of 1200°C, the $(BH)_{max}$ curves reach their peak of 3.9×10^6 gauss-oersted at a soaking time of about 2 hours. For longer soaking times, the $(BH)_{max}$ values fall due to lower values of intrinsic coercive force and the curves intersect those of 1180°C at soaking times of 5-6 hours. This behaviour is important industrially since it means that, by using different combinations of operational variables, specimens with similar maximum energy products but with different ceramic and other magnetic properties can be produced.

Another property that is also important from the production point of view is the shrinkage. The values of thickness shrinkage (S_t) were almost three times the values of diametral shrinkage (S_d). For the conditions employed in this study, S_d values were of the order of 10%. The behaviour of these shrinkages with respect to the variables investigated did not exhibit such clear trends as did that of the other ceramic and magnetic properties. In general, however, the relative thickness-to-relative diameter ratio, B/A^* , increases with increasing forming pressure and decreases with increasing sintering temperature and soaking time.

* B is defined as $(100-S_t)$ and A as $(100-S_d)$

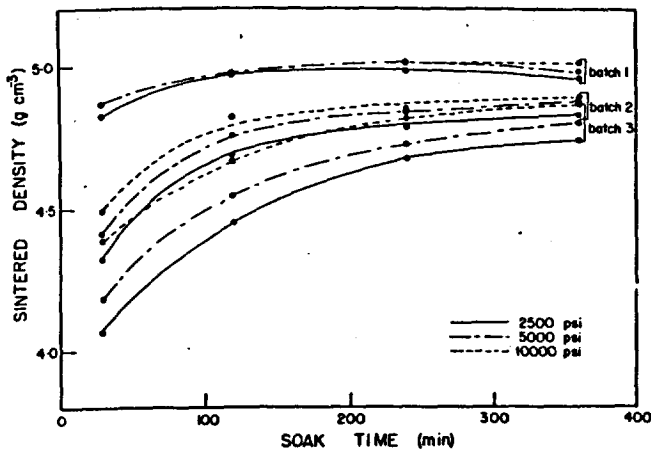


FIGURE 6. Effect of soak time and forming pressure on the sintered density of specimens prepared from batch Nos. 1, 2 and 3 of strontium ferrite, sintered at 1200°C.

Although batch Nos. 1, 2 and 3 show no apparent chemical differences, there are significant differences in the ceramic and magnetic properties of discs prepared from them. Figure 6 shows the sintered density of specimens prepared from these batches for various forming pressures and soaking times, all being sintered at 1200°C. The discs from batch No. 1 have higher density than those from batch Nos. 2 and 3. These differences decreased with increasing soaking time.

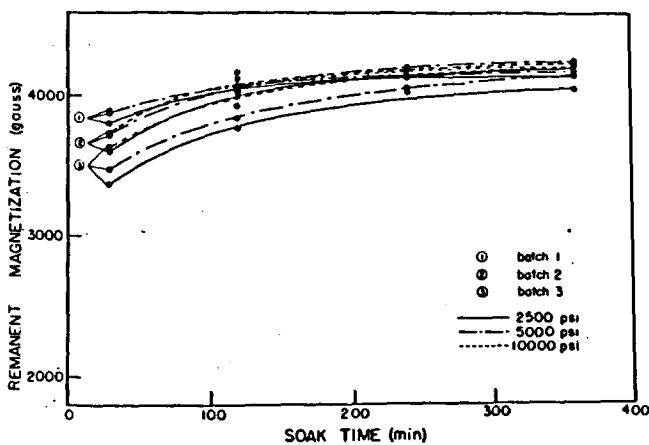


FIGURE 7. Effect of soak time and forming pressure on the remanent magnetization of specimens prepared from batch Nos. 1, 2 and 3 of strontium ferrite, sintered at 1200°C.

In Figure 7, it can be seen that the differences in remanent magnetization are not so apparent, especially for longer soaking times. It follows that, as can be seen in Figure 10, batch nos. 2 and 3 can produce discs with higher remanent magnetizations for a given density.

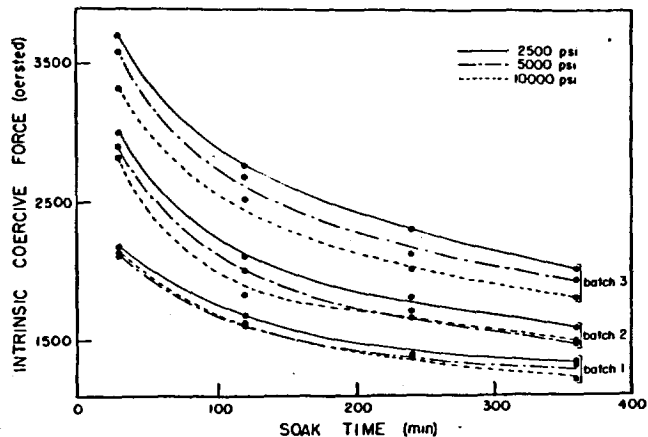


FIGURE 8. Effect of soak time and forming pressure on the intrinsic coercive force of specimens prepared from batch Nos. 1, 2 and 3 of strontium ferrite, sintered at 1200°C.

In Figure 8, it can be seen that the differences in intrinsic coercive force of the specimens prepared from these batches are more obvious and did not decrease as much with increasing soaking time. The discs from batch No. 3 have the highest values of intrinsic coercive force. Consequently, in view of the similarity in remanent magnetization noted above, a specimen prepared from batch No. 3 can potentially have the highest maximum energy product. Figures 8 and 9 show that, at a coercive force of 2000 oersted, maximum energy products of 3.6×10^6 gauss-oersted, 3.9×10^6 gauss-oersted and 4.1×10^6 gauss-oersted have been achieved for batch Nos. 1, 2 and 3, respectively.

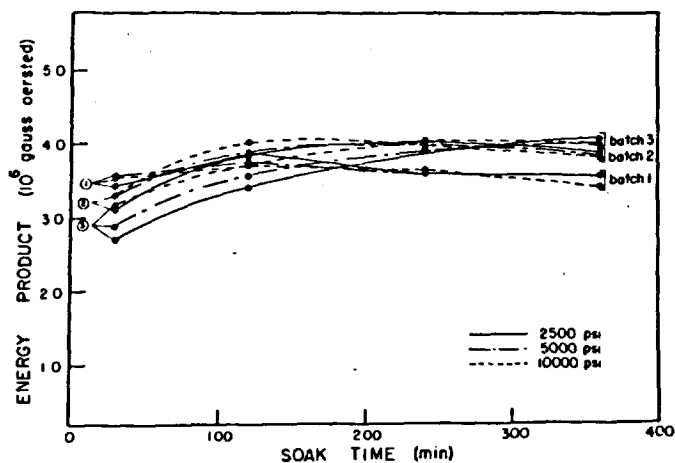


FIGURE 9. Effect of soak time and forming pressure on the maximum energy product of specimens prepared from batch Nos. 1, 2 and 3 of strontium ferrite, sintered at 1200°C.

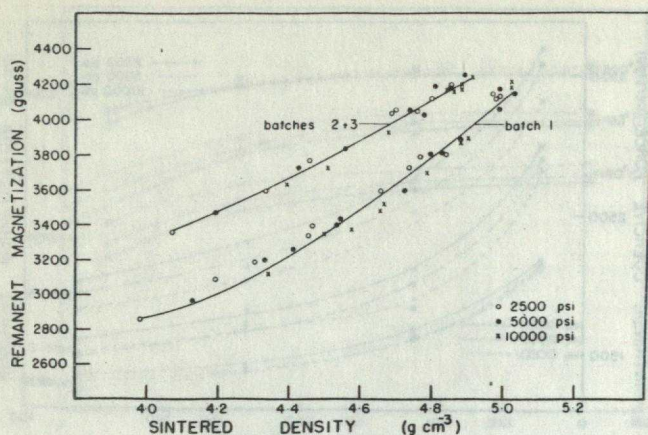


FIGURE 10. The relation between remanent magnetization and sintered density for all specimens prepared from batch Nos. 1, 2 and 3 of strontium ferrite.

Although the absolute values of these properties are not necessarily identical from batch to batch, their trends with respect to forming pressure, soaking time and, presumably, sintering temperature are very similar.

Conclusions

From the foregoing discussion it can be concluded that:

1. The forming pressure has a considerable effect on both the ceramic and magnetic properties of strontium ferrite magnets. This effect diminishes as the process of densification progresses.
2. The soaking time has a strong effect for short periods, but the values of the various properties approach an asymptote beyond 200 minutes. Since the properties are less sensitive to soaking time than to sintering temperature, it is simpler, from the control point of view, to use lower temperatures with longer times than vice versa in order to achieve the desired properties.

3. It is possible to produce ceramic magnets having similar maximum energy products but with different ceramic and other magnetic properties by using different combinations of operational variables.

4. It is difficult to obtain completely reproducible specimens from one batch to another. However, the reproducibility improves with the progress of sintering.

5. Maximum energy products as high as 4.1×10^6 gauss-oersted with a coercive force of 2000 oersted can be obtained with pure strontium ferrite ceramic magnets.

Acknowledgments

This investigation was conducted under the general direction of Dr. N.F.H. Bright, Head, Physical Chemistry Section. The authors are indebted to Dr. A.H. Webster, Physical Chemistry Section, for day-to-day discussions throughout the period of the work. The above-mentioned personnel are members of the staff of the Mineral Sciences Division, Mines Branch.

References

1. Sutarno, W.S. Bowman, G.E. Alexander, and J.D. Childs. The effect of some operational variables on the properties of strontium hexaferrite, *J. Can. Ceram. Soc.*, 38: 9-13, 1969.
2. Cochardt, A. Recent ferrite magnet development. *J. Appl. Phys.*, 37(3): 1112-1115, 1966.
3. Sutarno, W.S. Bowman, and G.E. Alexander. Ferrites: Part IV. The magnetic and ceramic properties of mixed barium-strontium ferrites. *Mines Branch Investigation Report IR 69-49*, 1969.
4. Shirk, B.T. *Dependence of coercive force on the intrinsic and extrinsic material properties of barium and strontium ferrite*. Ph.D. Thesis, The Pennsylvania State University, 1968.
5. Sutarno, W.S. Bowman, J.F. Tippins, and G.E. Alexander. Ferrites: Part III. Construction and operation of a magnetic orienting press for the fabrication of anisotropic ferrite magnets. *Mines Branch Investigation Report IR 67-46*, 1967.
6. Steingroever, E. Ein Magnetstahlprüfer mit Richtkraftkomponiertem Flussmesser. *Arch. Elektrotech.*, 40: 275-279, 1952.